Establishment of the mathematical model for diagnosing the engine valve faults by genetic programming

Wen-Xian Yang*

Institute of Vibration Engineering, Northwestern Polytechnical University, Xi'an 710049, China

Abstract

Available machine fault diagnostic methods show unsatisfactory performances on both on-line and intelligent analyses because their operations involve intensive calculations and are labour intensive. Aiming at improving this situation, this paper describes the development of an intelligent approach by using the Genetic Programming (abbreviated as GP) method. Attributed to the simple calculation of the mathematical model being constructed, different kinds of machine faults may be diagnosed correctly and quickly. Moreover, human input is significantly reduced in the process of fault diagnosis. The effectiveness of the proposed strategy is validated by an illustrative example, in which three kinds of valve states inherent in a six-cylinders/four-stroke cycle diesel engine, i.e. normal condition, valve-tappet clearance and gas leakage faults, are identified. In the example, 22 mathematical functions have been specially designed and 8 easily obtained signal features are used to construct the diagnostic model. Different from existing GPs, the diagnostic tree used in the algorithm is constructed in an intelligent way by applying a power-weight coefficient to each feature. The power-weight coefficients vary adaptively between 0 and 1 during the evolutionary process. Moreover, different evolutionary strategies are employed, respectively for selecting the diagnostic features and functions, so that the mathematical functions are sufficiently utilized and in the meantime, the repeated use of signal features may be fully avoided. The experimental results are illustrated diagrammatically in the following sections.
© 2005 Elsevier Ltd. All rights reserved.

1. Introduction

Many mechanical fault-diagnosing techniques based on vibration analysis have been fully developed over the last few decades [1]. Among them the well-known Fast Fourier Transform (FFT) is one of the most widely used and well-established methods. Based on the FFT, Qu et al. [2] developed an effective tool namely the Holospectrum for diagnosing rotating machinery and Yang et al. [3] successfully applied it to the diagnosis of a cracked rotor; unfortunately, the FFT-based methods failed to deal with non-stationary signals. Therefore, some time-frequency analysis methods such as Short Time Fourier Transform (STFT) [4], Wigner-Ville

---

*Corresponding author. Present address: Applied Mathematics and Computing Group, Department of Process and Systems Engineering, Cranfield University, Cranfield MK43 0AL, UK.

E-mail address: w.yang@cranfield.ac.uk.

Distribution (WVD) [5], Wavelet Transform (WT) [6] and the Instantaneous Power Spectrum (IPS) [7] were proposed and thereafter, their improved versions were further developed [8,9]. But few of them can meet the practical requirements completely with respect to on-line and intelligence performances because their operation needs human input and involve intensive calculations. For instance, the vibratory orbit of a rotor provides a useful clue for diagnosing the faults occurring in rotor-bearing system, but current computer programs cannot easily distinguish the orbit shapes automatically. Likewise, when diagnosing the faults in a rolling-element bearing, the quasi-periodic interval between neighbouring impulses in the signal is a very important indication that characterizes the type of bearing fault. But its automatic identification is also not easily programmed into a computer. In most cases, both the shape of rotor vibratory orbit and the aforementioned quasi-periodic interval in bearing signal are estimated by the means of visual observation or manual measurement. Sometimes, however, manual methods cannot work effectively, in particular, when diagnosing the machinery with complex structures such as diesel engines. In these cases, the vibratory features characterizing different kinds of faults overlap together, so that engineers cannot diagnose the faults at all from the direct observation of the signals. In order to tackle this difficulty in the diagnosis of faults inherent in complex machinery, an intelligent approach has been developed in this study using the Genetic Programming (abbreviated as GP) method.

The GP was first clearly defined by Koza [10]. It involves finding both the functional form (the structure of the tree) and the numeric coefficients (terminals) for the model. In comparison with the conventional Genetic Algorithm (GA) [11], its individual component parts are represented by binary trees and terminals rather than by coded strings of numbers. As GP allows the optimization of much more complex structures, it can therefore be applied to a greater diversity of problems [12–14]. Recently, Chen et al. [7] adopted it to diagnose the faults occurring in rolling-elements bearings. However, most of the available GPs use a few predefined binary tree structures and a small number of basic mathematical operators (e.g. $+$, $-$, $\times$, $\div$ and power). Moreover, every terminal plays an equal role in the model. This is not true in reality and affects the flexibility of the optimization. In view of the aforementioned insufficiencies of existing GPs, a new GP approach is proposed in this paper. Using this proposed GP approach, many more mathematical functions, instead of the basic operators, will be introduced and the diagnostic tree will be constructed intelligently by applying an adaptive power-weight coefficient to each terminal (i.e. signal features). The structure of the tree is optimized adaptively with the variation of the power-weight coefficients between 0 and 1. In addition, different evolutionary strategies will be employed, respectively for the selections of the functions and signal features, so that the designed functions may be sufficiently utilized whilst in the meantime, the repeated use of signal features can be completely avoided. A group of constant numbers will be employed to avoid the occurrence of morbid solutions. In the paper, the effectiveness and feasibility of the proposed approach will be verified by an example where a mathematical model has been designed to diagnose the running states of an exhaust valve in a six-cylinders/four-stroke cycle diesel engine. The remaining parts of the paper are organized as follows.

In Section 2, the characteristics of both the vibratory signals collected from the exhaust valve and the corresponding cylinder pressure signals are analysed, based on which 8 signal features are considered to be the possible terminals of the diagnostic tree. Moreover, the same number of power-weight coefficients are designed simultaneously, from which the importance of the role of every feature in the mathematical model is indicated.

In Section 3, the 22 mathematical functions or 'operators' are deliberately designed for constructing the diagnostic tree. In the meantime, the same number of constants are used in order to avoid the occurrence of morbid solutions (e.g. the quantity in the model is divided by zero).

In Section 4, the fitness function that drives the evolutionary process is designed. Meanwhile, different evolutionary strategies are applied to the selections of the features, the 'operators' and the power-weight coefficients as well as the constant numbers, respectively.

In Section 5, using the specially designed GP program, the diagnostic tree is optimized adaptively until either the pre-defined maximum iteration time is reached or the satisfied fitness value is achieved. The optimized diagnostic tree is eventually formulated into a mathematical equation.

Finally, the effectiveness of the mathematical model identifying the running states of an engine valve is demonstrated by an illustrative experiment in Section 6.

2. Characteristics of engine signals

Nowadays, the need to further improve the diagnostic technique of engine faults has been widely recognized, but due to the complex structure and the presence of multi-excitation sources, the vibratory signals collected from engines are complicated in composition. Moreover, the features of the signals collected in different fault conditions often overlap together with each other. Thus, the engine faults are very difficult to diagnose by convenient means. Fig. 1 shows the vibratory signals collected from an exhaust valve of a six-cylinders/four-stroke cycle diesel engine. The valve works under three different conditions, (1) the normal condition, (2) the valve-tappet clearance faulty condition and (3) the gas leakage fault condition. The normal valve clearance is 0.1 mm and in the experiments, a severe valve clearance fault was simulated and the clearance was adjusted to be 0.5 mm. The gas leakage fault was simulated by producing a 3 mm long crack on the cap of the valve. Two kinds of signals were considered in the calculation, one was the vibration signal collected from the cap of the exhaust valve and another was the cylinder pressure. The latter was measured using a pressure sensor fitted to an adapted cylinder pressure indicator port that would normally be terminated with a mechanical pressure gauge. This arrangement proved convenient as it was not possible to install a pressure sensor directly in the combustion chamber of the engine. The sampling frequency was 25 kHz and during the data acquisition process, the rotating speed of the engine was kept at a constant 1500 rpm.

From Fig. 1, it was found that the signals collected under different valve running conditions showed different complexities in structure. But the signal at every stage appeared similar in the form of the impulses with decaying amplitudes and periods, despite the running states of the valve. Among the five stages, the fourth stage showed the strongest vibration. Moreover, the vibration at each stage increased or decreased more or less when the valve worked abnormally. Based on these observations the following criteria were designed for characterizing the signals. If it was assumed that the time series signal is x_i ($i = 1, 2, \ldots, N$), then

(1) General vibration intensity E_1:

$$E_1 = \sqrt{\sum_{i=1}^{N} x_i^2 / N},$$

(1)

where N denotes the number of data.

(2) Vibration intensity at the second stage E_2:

$$E_2 = \sqrt{\sum_{i=l}^{m} x_i^2 / (m - l + 1)},$$

(2)

where l and m indicate the first and the last number of data collected at the second stage, respectively.

(1) the exhaust valve closes; (2) the inlet valve closes; (3) gas combustion burst;
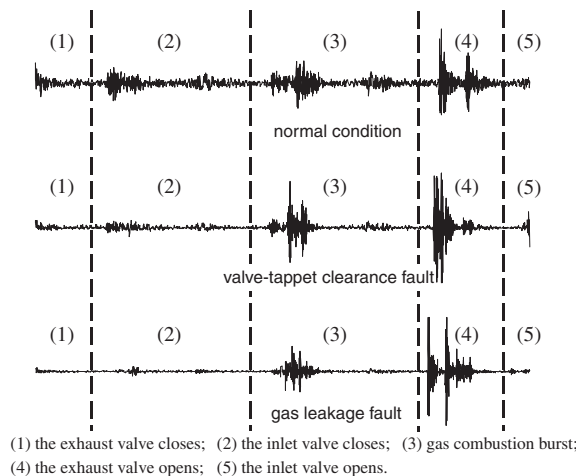(4) the exhaust valve opens; (5) the inlet valve opens.

Fig. 1. Vibration signal collected from the exhaust valve of the engine.

(3) Vibration intensity at the third stage E_3:

$$E_3 = \sqrt{\sum_{i=m+1}^{n} x_i^2 / (n - m + 2)}, \tag{3}$$

where n indicates the last number of data collected at the third stage.

(4) Structural complexity S:

$$S = -\sum_{i=1}^{\Omega} \frac{N_i'}{N} \log_2 \left(\frac{N_i'}{N} \right), \tag{4}$$

where S, in essence, is the structural entropy of the signal. Herein, the amplitude region of the signal is divided into Ω sub-regions. N_i' ndicates the number of the data located in the ith sub-region.

From the long-term observations, it was also found that the vibratory energy of the valve was redistributed in the frequency domain when the valve worked abnormally, as shown in Fig. 2. It is necessary to note that the sub-plots in Fig. 2 are the frequency spectra of those signals shown in Fig. 1.

From Fig. 2, it was observed that when the valve worked abnormally, the vibration energy moved forward towards the high-frequency region (i.e. larger than 9 kHz) and in consequence, the low-frequency vibration decreased correspondingly at the same time. The observation showed that the remarkable differences among the spectra occurred in the regions (6.5 kHz, 9 kHz) and (9 kHz, 12.5 kHz), respectively. In order to characterize these phenomena, the fifth and the sixth criteria were designed.

(5) The ratio of the vibration in the region from 6.5 to 9 kHz, R_1:

$$R_1 = \frac{\sum_{i=a}^{b} d_i}{\sum_{j=1}^{N} d_j}, \tag{5}$$

where d_j ($j = 1, 2, \ldots, i, \ldots, N$) are the spectral data derived by the FFT, and a and b represent the first and the last number of spectral data in the region (6.5 kHz, 9 kHz), respectively.

(6) The ratio of the vibration in the region from 9 to 12.5 kHz, R_2:

$$R_2 = \frac{\sum_{i=b}^{N} d_i}{\sum_{j=1}^{N} d_j}. \tag{6}$$

In order to see whether these vibratory criteria can really work in identifying the running states of the valve, Fig. 3 plots their calculated results obtained during a series of experiments.
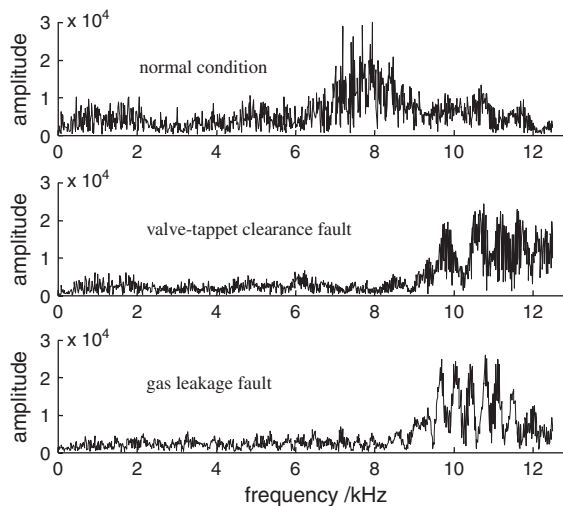

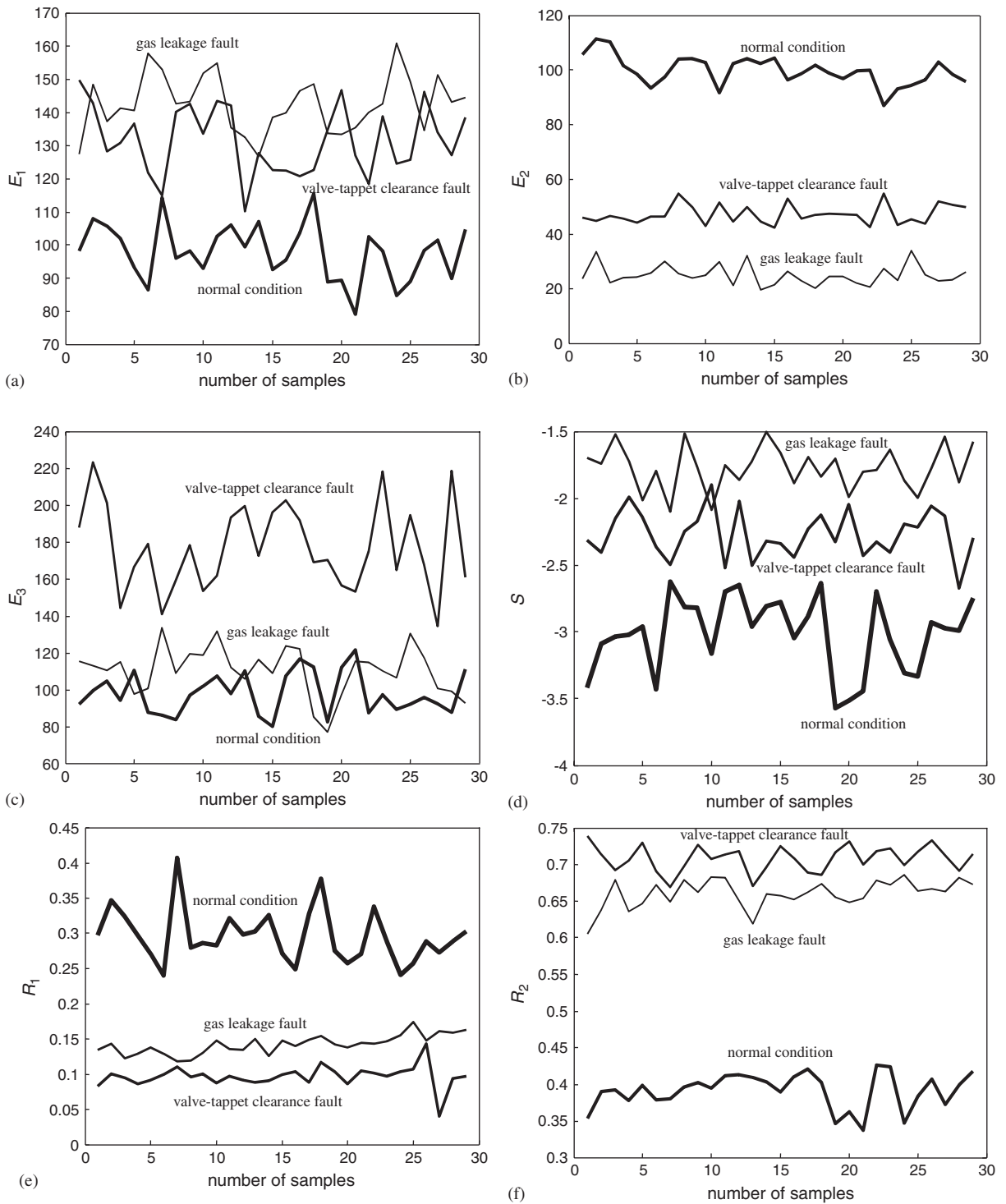Fig. 2. The frequency spectra of the signals shown in Fig. 1.

Fig. 3. Computational results of the six vibratory criteria. (a) E_1, (b) E_2, (c) E_3, (d) S, (e) R_1, and (f) R_2.

From Fig. 3, it was found that the vibratory criteria, derived under different valve running conditions, either overlapped together or were very close to each other. Obviously, they cannot be directly applied to the identification of valve states, but from Eqs. (1)–(6), it is seen that these criteria are much more easily obtained than those used by Chen et al. [7].
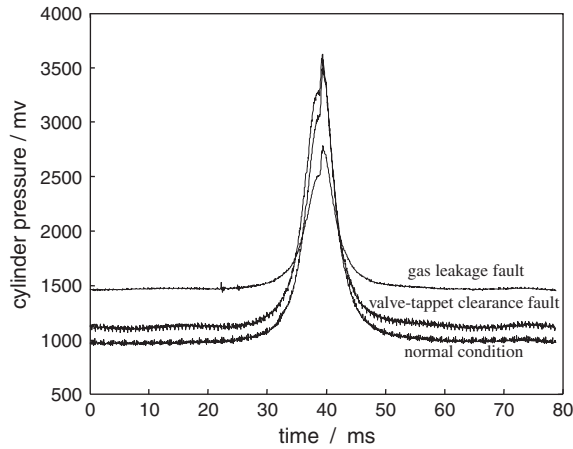
Fig. 4. Cylinder pressure signals collected under different running conditions of the valve.

Experiments revealed that cylinder pressure was also an important feature for diagnosing valve states, as shown in Fig. 4. From this figure, it is clearly seen that when the running state of the valve has changed especially when a gas leakage fault occurs, the maximum value of the cylinder pressure will change significantly. Moreover, the decreasing ratio of the cylinder pressure in one working cycle is modified as well.

Based on the above observations, the seventh and eighth features were further designed.

(7) The maximum cylinder pressure $P_{\max}$:

$$P_{\max} = \max(p_i | i = 1, 2, \ldots, M), \tag{7}$$

where M indicates the number of data included in the cylinder pressure signal p_i ($i = 1, 2, \ldots, M$).

(8) The decreasing ratio R_p of the cylinder pressure signal:

$$R_p = \frac{\Delta P}{P_{\max}}. \tag{8}$$

The $P_{\max}$ and ΔP are illustrated in Fig. 5. Their calculation results derived during experiments are shown in Fig. 6.

From Fig. 6, it is seen that the $P_{\max}$ derived under different valve conditions overlap together with each other and so does the R_p. Numerical results, shown in Figs. 3 and 6, suggest that the valve states cannot be identified correctly by directly using the calculated results of these criteria. This is why a new approach has been developed and described in this paper.

Using the aforementioned 8 criteria, the set of features for constructing the diagnostic tree is written as a 3×8 matrix $\mathbf{F} = [\mathbf{E}_1, \mathbf{E}_2, \mathbf{E}_3, \mathbf{S}, \mathbf{R}_1, \mathbf{R}_2, \mathbf{P}_{\max}, \mathbf{R}_p]$, where, $\mathbf{E}_1 = [E_1' \quad E_1'' \quad E_1''']'$. E_1', E_1'' and E_1''' are the E_1, respectively derived at three different kinds of valve states. The other features in the matrix $\mathbf{F}$ have similar expressions.

In addition, the research carried out in Ref. [15] reveals that different signal features play different roles in fault diagnosis. In other words, some features play more important roles, while others play less important roles or even, in some cases, do not play any role in the diagnosis. In view of this, a particular set of power-weight coefficients $\mathbf{C} = \{0 \leqslant c_i \leqslant 1 | i = 1, 2, \ldots, 8\}$ was further designed. They corresponded to the aforementioned 8 criteria, and indicate the importance of the roles that these criteria play in the construction of the diagnostic tree. With the aid of $\mathbf{C}$, the flexibility of the optimization of the diagnostic tree is dramatically improved. For example, in case of $c_i = 0$, the ith feature in the set of terminals $\mathbf{F}$ does not play any role in the tree, so the binary tree related to this feature can be cut off from the main trunk. Conversely, the binary trees related to those features with $c_i \neq 0$ ($i = 1, 2, \ldots, 8$) will be reserved.
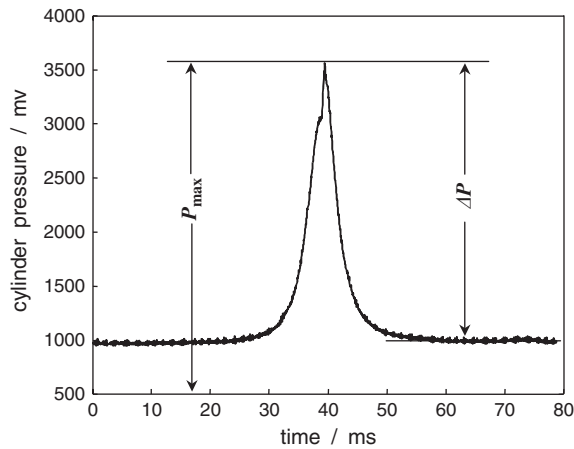
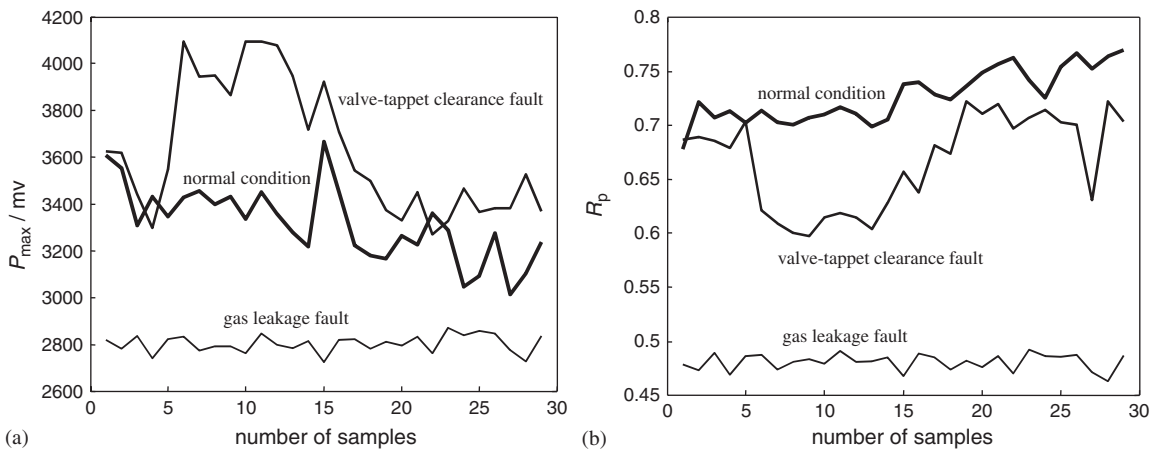Fig. 5. Cylinder pressure signatures P_{max} and ΔP.

Fig. 6. Calculation results of P_{max} and R_p (a) P_{max}, (b) R_p.

3. Mathematical functions

Instead of using a few basic operators adopted by conventional GPs, a series of mathematical functions are taken as the 'operators' in the proposed GP so that more complex mathematical computation forms can be involved in the optimization process. The designed 'operators' are listed in Table 1.

In the functions, y_j is the result derived from the jth iterative calculation. f_i represents the ith feature in the set of terminals **F**. c_i denotes the power-weight coefficient corresponding to f_i. In addition, a group of constant numbers $\varepsilon = \{0 < \varepsilon_i \leqslant 1 | i = 1, 2, \ldots, 8\}$ was also designed for avoiding the occurrence of morbid solutions. The coded constant numbers in the set ε_i ($i = 1, 2, \ldots, 8$) can be optimized as well. From Table 1, it should be noticed that in designed 'operators', the feature f_i is multiplied by the power-weight coefficient c_i first before carrying out further calculations of the function, so that the roles of the features play in the mathematical model are taken into account in the calculation. Moreover, through optimizing c_i ($i = 1, 2, \ldots, 8$), the structure of the diagnosing tree may be optimized adaptively whilst in contrast, the convenient GPs do not possess this merit. The diagram of the diagnostic tree is shown in Fig. 7.

In this figure, the composite criterion w is finally derived from the diagnostic tree, which can be taken as the measure for identifying the running states of the valve.

Table 1
Mathematical functions

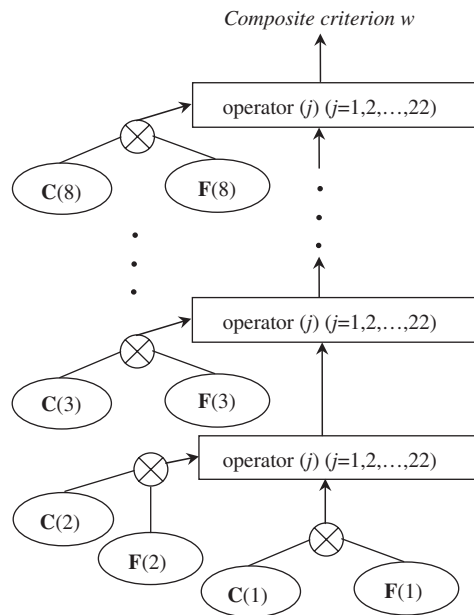| No.	Functions	No.	Functions
1	$y_{j+1} = c_i f_i + y_j$	12	$y_{j+1} = \sqrt{|y_j/(\varepsilon_i + c_i f_i)|}$
2	$y_{j+1} = c_i f_i - y_j$	13	$y_{j+1} = \sqrt{|c_i f_i|} + y_j$
3	$y_{j+1} = c_i f_i y_j$	14	$y_{j+1} = c_i f_i + \sqrt{|y_j|}$
4	$y_{j+1} = |c_i f_i y_j|$	15	$y_{j+1} = \sqrt{|c_i f_i|} - y_j$
5	$y_{j+1} = c_i f_i/(\varepsilon_i + y_j)$	16	$y_{j+1} = c_i f_i - \sqrt{|y_j|}$
6	$y_{j+1} = \sqrt{|c_i f_i + y_j|}$	17	$y_{j+1} = y_j \sqrt{|c_i f_i|}$
7	$y_{j+1} = \sqrt{|c_i f_i - y_j|}$	18	$y_{j+1} = c_i f_i \sqrt{|y_j|}$
8	$y_{j+1} = \sqrt{|c_i f_i y_j|}$	19	$y_{j+1} = \sqrt{|c_i f_i|}/(\varepsilon_i + y_j)$
9	$y_{j+1} = \sqrt{|c_i f_i/(\varepsilon_i + y_j)|}$	20	$y_{j+1} = c_i f_i/\left(\varepsilon_i + \sqrt{|y_j|}\right)$
10	$y_{j+1} = y_j - c_i f_i$	21	$y_{j+1} = (c_i f_i)^2 + y_j$
11	$y_{j+1} = y_j/(\varepsilon_i + c_i f_i)$	22	$y_{j+1} = c_i f_i + y_j^2$

Fig. 7. The diagram of the diagnosing tree.

4. Evolutionary strategies

During the evolutionary process, four factors will be involved in the optimization. They are the orders of the features in the set **F**, the coded coefficients in the set **C**, the coded constant numbers in the set **ε** as well as the orders of the functions in the set of 'operators', respectively. For the last three factors, their evolution will be realized by performing the conventional crossover and mutation operations. The details of the crossover and mutation operations may be found from Ref. [11]. But the optimization of the orders of the features cannot be manipulated in the same way, otherwise the features in the set **F** could be used repeatedly. In essence, the optimization of the orders of the features belongs to the type of travelling salesman problems (TSPs). The related description about the TSPs may be found in Ref. [16]. Whilst aiming at solving the TSPs by using genetic algorithms, the author has been innovative and proposed an improved genetic operator namely 'Immigration Operator (IO)' [17]. A brief introduction of the IO is given as follows.
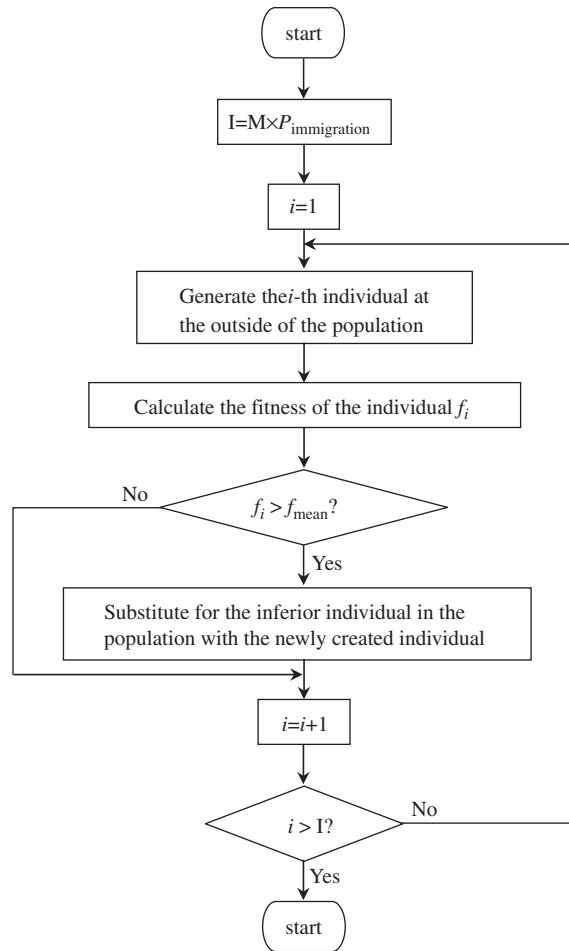
Fig. 8. The operating scheme of the IO.

The IO is a special strategy for generating individuals at the outside of the population and then introducing the fitter ones into the population to substitute for those inferior individuals. The operating scheme of the IO is depicted in Fig. 8, where, M represents the scale of the population, $P_{\mathrm{immigration}}$ the probability of immigration operation, I the number of individuals that will be generated, f_i the fitness value of the ith individual, and f_{mean} the mean fitness of the individuals contained in present population.

As depicted in Fig. 8, the individuals are generated stochastically, but the population will not accept all individuals being generated. Only those with the fitness larger than the mean fitness of the available individuals contained in present population may be regarded as the "qualified ones". Hence, the individuals accepted by the population possess better fitness. This is why the IO can drive the evolution of the population more efficiently. Other merits of the IO may be found from Ref. [17].

Using different evolutionary strategies, the GP program was designed and its operating diagram is shown in Fig. 9.

In order to accomplish a perfect classification of different valve states, both the largest pseudo-space distances among different groups of samples and the smallest pseudo-space distances among different samples contained in the same group are considered simultaneously. The fitness function for the GP is designed as

$$f = \frac{\sum_{j,k=1,j \neq k}^{a} \left[\sum_{i,l=1}^{b} (w_{ij} - w_{lk}) \right]}{\sum_{k=1}^{a} \left[\sum_{i,l=1,i \neq l}^{b} (w_{ik} - w_{lk}) \right]}, \tag{9}$$
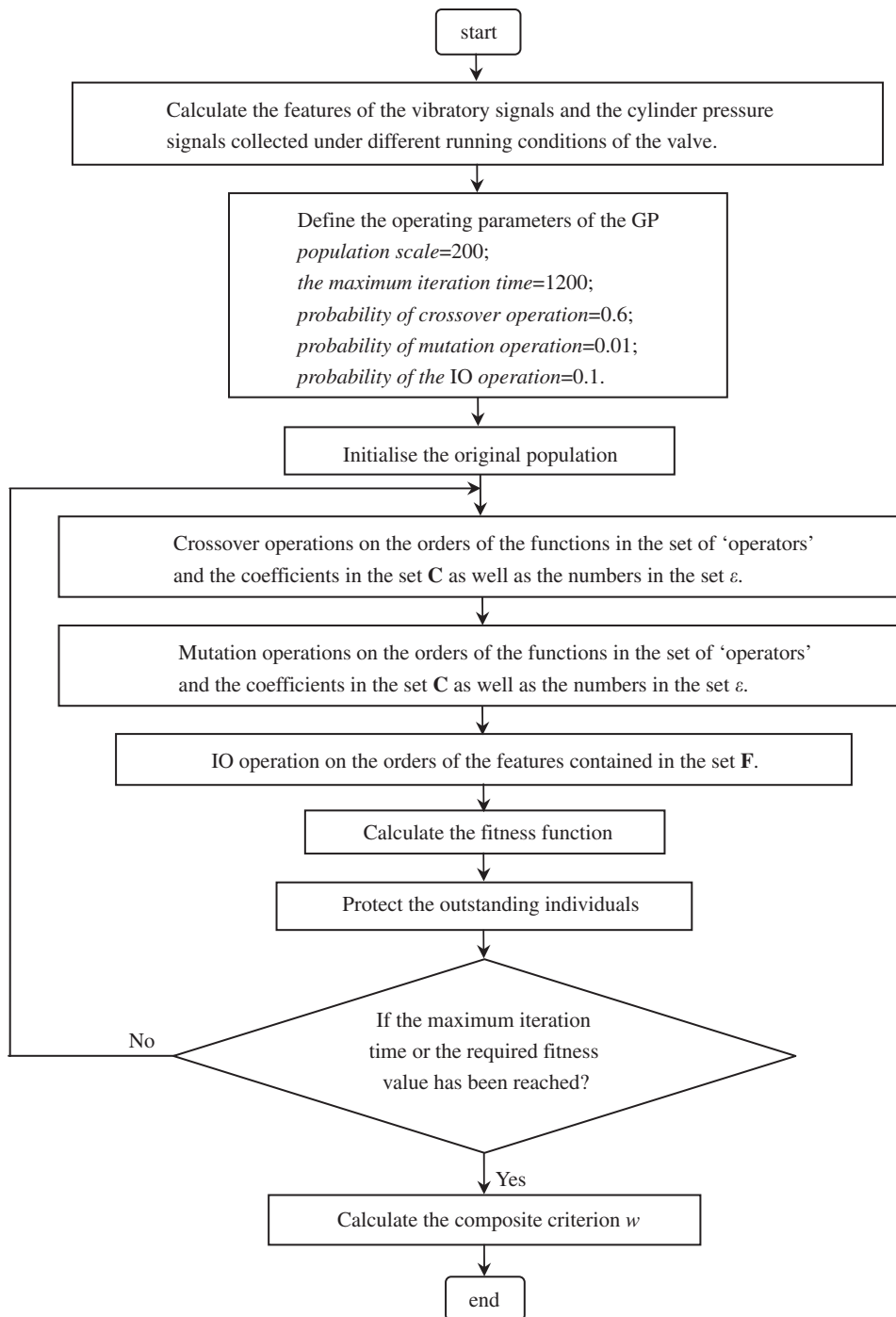
Fig. 9. The operating diagram of the GP.

where a indicates the number of valve states being considered, b the number of signals collected at each valve state w_{ij} denotes the composite criterion derived from the ith signal collected under the jth running state of the valve. w_{lk} and w_{ik} have similar meanings.

5. The implementation of the GP

Adopting the GP algorithm depicted in Fig. 9 and taking the fitness function f described by Eq. (9) as the measure for evaluating the fitness levels of the individuals, the diagnostic tree, shown in Fig. 7, is optimized for diagnosing three such kinds of valve running states as (1) the normal condition, (2) the valve-tappet clearance fault and (3) the gas leakage fault. The recorded evolutionary history is shown in Fig. 10.

The optimized results are listed in Table 2.

After substituting the optimized results listed in Table 2 into the diagnostic tree, the following mathematical model for identifying the valve state is readily derived:

$$w = \frac{0.6745^2 \times R_p \times P_{\max}}{0.5746 + 0.0515 \times S + \left[\left|\dfrac{0.1540 \times R_1}{0.0279 + \left(\left|\frac{|0.5351 \times R_2/0.6619|^{1/2} - 0.0212 \times E_2|}{0.9965 + 0.6745 \times E_3}\right|\right)^{1/2}}\right|\right]^{1/2}}$$

$$= \frac{0.4550 \times R_p \times P_{\max}}{0.5746 + 0.0515 \times S + \left[\left|\dfrac{0.1540 \times R_1 \times |0.9965 + 0.6745 \times E_3|^{1/2}}{0.0279 \times |0.9965 + 0.6745 \times E_3|^{1/2} + \left(|0.8991 \times |R_2|^{1/2} - 0.0212 \times E_2|\right)^{1/2}}\right|\right]^{1/2}}. \tag{10}$$

From Eq. (10), it is noticed that only 7 features appear in the mathematical model, though 8 criteria were considered during the optimization. This is because the first function in the optimized result is $y_{j+1} = \sqrt{|c_i f_i y_j|}$ (refer to Tables 1 and 2). As at the beginning of the GP, the initial value of y_j is zero, this function does not play any role in the model and the role of the first feature in the optimized set $\mathbf{F}$ is ignored. From Table 2, it is found that this feature is E_1. That is also why E_1 does not appear in the final mathematical model.
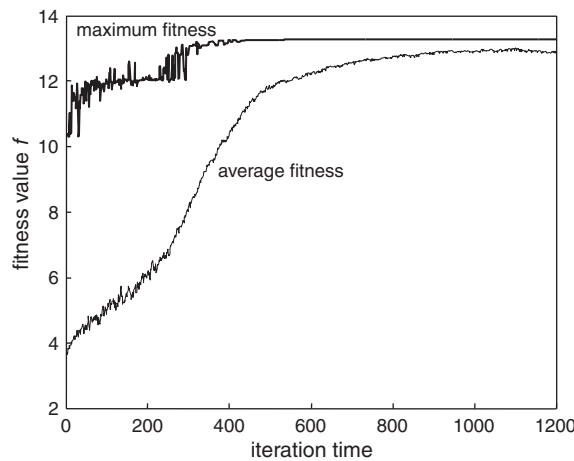

Fig. 10. The recorded evolutionary history.

Table 2
Optimized results

Items	Optimized results
The orders of the features in the set **F**	{1, 6, 2, 3, 5, 4, 8, 7}
The coefficients in the set **C**	{0.1526, 0.5351, 0.0212, 0.6745, 0.1540, 0.0515, 0.6745, 0.6745}
The constant numbers in the set **ε**	{0.3647, 0.6619, 0.5746, 0.9965, 0.0279, 0.4955, 0.5746, 0.3860}
The orders of the functions in the set of 'operators'	{8, 9, 10, 11, 20, 14, 5, 3}

6. Application of the mathematical model in the diagnosis of valve states

Aiming at demonstrating the effectiveness of the derived mathematical model in identifying the running states of the valve, 29 additional signals were collected under each kind of valve running condition. After extracting the features specified by set **F** from the sample data, the features were substituted into Eq. (10). The Composite Criterion w was calculated and the results were plotted in Fig. 11.

Fig. 11 shows that using the mathematical model derived by the GP, the three different kinds of valve states are distinguished correctly and efficiently. The overlapping phenomenon among them does not occur at all on the composite criterion w. In order to further prove the merit of the derived mathematical model on valve state classification, the following experiments were also carried out for comparison.

The Principal Component Analysis (PCA) method has been widely accepted as a favoured tool for constructing the classification models [15]. Hence, the PCA was also employed to solve the present problem. The numerical results of the first, the second and the third orders of principal components (PC1–PC3) derived by the PCA are given in Fig. 12.

From Fig. 12, it is easily found that using the mathematical model derived from the PCA method, the three kinds of valve states cannot be distinguished satisfactorily because of the overlapping phenomenon existing among them. The accuracy of the classification may be improved by employing the Kernel Principal Component Analysis (KPCA) method [15], but in the case of using KPCA, the mathematical model is difficult to establish as the nonlinear operation is involved in the computing algorithm.

7. Concluding remarks

From the aforementioned research studies, the merits of the proposed GP approach may be summarized as follows:

(1) In comparison with the features adopted by Chen et al. [7], the signal features used in the proposed GP are more easily obtained. No further complex calculation is needed.
(2) The introduction of the power-weight coefficients into the GP allows the optimization of the diagnostic tree to be a more logical process, dramatically improving the flexibility of the optimization.
(3) The use of different evolutionary strategies fully ensures sufficient utilization of both the signal features and the 'operators'. Incorporating the constant numbers introduced, the morbid solutions are completely avoided.
(4) The proposed GP approach produces a simple, feasible and effective mathematical model for diagnosing the running states of the engine valve. However, such a perfect model is difficult to achieve by using conventional signal processing methods like wavelet transform or other advanced signal processing tools.
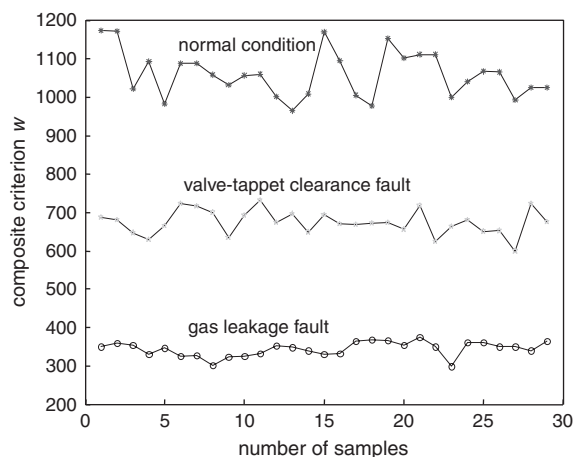

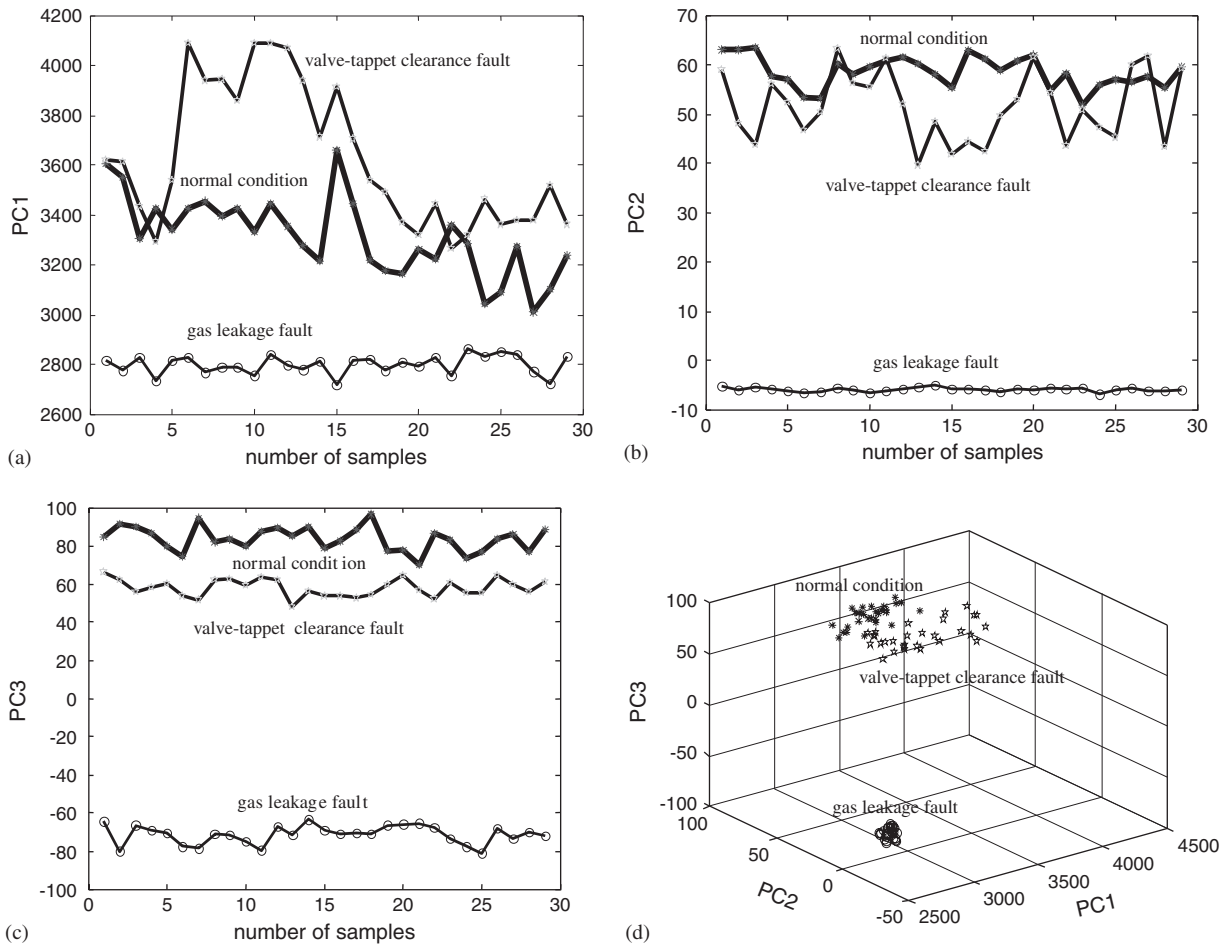Fig. 11. The results derived by the mathematical model.

Fig. 12. The results derived by the PCA method. (a) PC1, (b) PC2, (c) PC3, and (d) three dimensional plot PC1–PC2–PC3.

(5) The simple calculation of the signal features and the mathematical model make it much easier to realize an intelligent online fault diagnostic system.

(6) Compared with the PCA or other conventional classification methods, the proposed GP technique shows more powerful ability in solving the classification problems.

Acknowledgements

References

[1] Z.K. Peng, F.L. Chu, Application of the wavelet transform in machine condition monitoring and fault diagnostics: a review with bibliography, Mechanical System and Signal Processing 18 (2004) 199–221.

[2] L.S. Qu, X. Liu, Y.D. Chen, The holospectrum: a new method for rotating surveillance and diagnosis, Journal of Mechanical Signature and Signal Processing 3 (3) (1989) 255–268.

W.-X. Yang / Journal of Sound and Vibration 293 (2006) 213–226

[3] W.X. Yang, L.S. Qu, J.S. Jiang, Study of the diagnostic features of a rotor with a transverse crack, *INSIGHT-Non-Destructive and Condition Monitoring (The Journal of the British Institute of Non-Destructive Testing)* 43 (8) (2001) 537–545.

[4] I.S. Koo, W.W. Kim, Development of reactor coolant pump vibration monitoring and a diagnostic system in a nuclear power plant, *ISA Transactions* 39 (2000) 309–316.

[5] P.C. Russell, J. Cosgrave, D. Tomtsis, A. Vourdas, L. Stergioulas, J.R. Jones, Extraction of information from acoustic vibration signals using Gabor Transform type devices, *Measurement Science and Technology* 9 (1998) 1282–1290.

[6] W.J. Staszewski, Structural and mechanical damage detection using wavelets, *The Shock and Vibration Digest* 30 (1998) 457–472.

[7] P. Chen, M. Taniguchi, T. Toyota, Z.J. He, Fault diagnosis method for machinery in unsteady operating condition by instantaneous power spectrum and genetic programming, *Mechanical System and Signal Processing* 19 (2005) 175–194.

[8] A. Francois, F. Patrick, Improving the readability of time-frequency and time-scale representations by the reassignment method, *IEEE Transactions on Signal Processing* 43 (1995) 1068–1089.

[9] P.W. Tse, W.X. Yang, H.Y. Tam, Machine fault diagnosis through an effective exact wavelet analysis, *Journal of Sound and Vibration* 277 (2004) 1005–1024.

[10] J.R. Koza, Genetic programming: on the programming of computers by means of natural selection, A Bradford Book, MIT Press, Cambridge, MA, 1992.

[11] J. Holland, *Adaptation in Natural and Artificial Systems*, University of Michigan Press, Ann Arbor, 1975.

[12] C.D. Stefano, A.D. Cioppa, A. Marcelli, Character preclassification based on genetic programming, *Pattern Recognition Letters* 23 (2002) 1439–1448.

[13] M.L. Wong, A flexible knowledge discovery system using genetic programming and logic grammars, *Decision Support Systems* 31 (2001) 405–428.

[14] P.A. Whigham, P.F. Crapper, Modelling rainfall-runoff using genetic programming, *Mathematical and Computer Modelling* 33 (2001) 707–721.

[15] W.X. Yang, Vibration-based diagnosis of engine valve faults, *INSIGHT-Non-Destructive and Condition Monitoring (The Journal of the British Institute of Non-Destructive Testing)* 45 (8) (2003) 1–7.

[16] R. Yang, Solving Large Travelling Salesman Problems with Small Population, International Conference on Genetic Algorithms in Engineering Systems: Innovations and Application, University of Strathclyde, Glasgow, UK, 1997, pp. 157–162.

[17] W.X. Yang, An improved genetic algorithm adopting immigration operator, *International Journal of Intelligent Data Analysis* 8 (4) (2004) 385–401.